


Microwave Dielectric Properties of $(\text{Ba}_{1-x}\text{Na}_x)(\text{Mg}_{0.5-2x}\text{Y}_{2x}\text{W}_{0.5-x}\text{Ta}_x)\text{O}_3$ Ceramics

Chang-Bae Hong*, Shin Kim**, Sun-Ho Kwon*, and Sang-Ok Yoon **†

*Department of Materials Engineering, Graduate School, Gangneung-Wonju National University, Gangneung 25457, Korea

**Department of Advanced Ceramic Materials Engineering, Gangneung-Wonju National University, Gangneung 25457, Korea

(Received July 1, 2019; Revised July 16, 2019; Accepted July 16, 2019)

ABSTRACT

The phase evolution, microstructure, and microwave dielectric properties of $(\text{Ba}_{1-x}\text{Na}_x)(\text{Mg}_{0.5-2x}\text{Y}_{2x}\text{W}_{0.5-x}\text{Ta}_x)\text{O}_3$ ($0 \leq x \leq 0.05$) ceramics were investigated. All compositions exhibited a 1:1 ordered perovskite structure. As the value of x increased, the dielectric constant (ϵ_r) exhibited a tendency to increase slightly. The quality factor reached the maximum value at $x = 0.01$. The temperature coefficient of resonant frequency (τ_f) increased from -19.32 ppm/ $^\circ\text{C}$ to -5.64 ppm/ $^\circ\text{C}$ in the positive direction as x increased. The dielectric constant (ϵ_r), quality factor ($Q \times f_0$), and temperature coefficient of resonant frequency (τ_f) of the composition $x = 0.05$, i.e., $(\text{Ba}_{0.95}\text{Na}_{0.05})(\text{Mg}_{0.4}\text{Y}_{0.1}\text{W}_{0.45}\text{Ta}_{0.05})\text{O}_3$ were 19.9, 128,553 GHz, and -5.6 ppm/ $^\circ\text{C}$, respectively.

Key words : $\text{Ba}(\text{Mg}_{0.5}\text{W}_{0.5})\text{O}_3$, Ordered perovskite, Dielectric constant, Quality factor, Temperature coefficient of resonant frequency

1. Introduction

According to the rapid growing of commercial wireless communication industry, many works of microwave dielectric ceramics used for mobile phone, wireless LAN (local area network), GPS (global position satellite), and ITS (intelligent transport system) are being actively conducted.¹⁻³⁾ For applications in resonators, filters, and oscillators at microwave frequencies, microwave dielectric ceramics should have high dielectric constant (ϵ_r) for miniaturization, high quality factor ($Q \times f_0$) for high frequency selectivity, and nearly zero temperature coefficient of resonant frequency (τ_f) for thermally stable circuits.⁴⁾

Among the various dielectric resonators at microwave frequencies such as $\text{Ba}(\text{M}_{0.33}\text{Ta}_{0.67})\text{O}_3$ (where $\text{M} = \text{Mg}^{2+}$ and Zn^{2+}) with 1:2 ordered structure of B-site cations in the perovskite,^{5,6)} $\text{Ba}(\text{Mg}_{0.5}\text{W}_{0.5})\text{O}_3$ (BMW) having the ordered perovskite structure, in which B-site cations are 1:1 ordered because their large difference in size and charge, has been investigated since Takahashi et al. reported that the dielectric properties of BMW are $\epsilon_r = 16.7$, $Q \times f_0 = 42,000$ GHz, and $\tau_f = -33.6$ ppm/ $^\circ\text{C}$.⁷⁻¹⁰⁾ Bian et al. reported that the composition of $x = 0.3$ in the $\text{Ba}[\{\text{Mg}_{(1-x)/2}\text{Y}_{x/3}(\text{V}_{\text{Mg}/6})\}\text{W}_{1/2}]\text{O}_3$ system exhibited the dielectric properties $\epsilon_r = 21.9$, $Q \times f_0 = 133,000$ GHz, and $\tau_f = -2.4$ ppm/ $^\circ\text{C}$.⁹⁾ Lin et al. investigated the microwave dielectric properties of the $(\text{Ba}_{1-x}\text{Sr}_x)$ -

$(\text{Mg}_{0.5}\text{W}_{0.5})\text{O}_3$ system, and found that the composition of $x = 0.25$ had the dielectric properties $\epsilon_r = 20.6$, $Q \times f_0 = 152,600$ GHz, and $\tau_f = +24$ ppm/ $^\circ\text{C}$.⁹⁾ Wu et al. reported that the composition of $x = 0.02$ in the $(1-x)\text{Ba}(\text{Mg}_{0.5}\text{W}_{0.5})\text{O}_3$ - $(x)\text{Ba}(\text{Y}_{0.67}\text{W}_{0.33})\text{O}_3$ system exhibited the dielectric properties $\epsilon_r = 20$, $Q \times f_0 = 160,000$ GHz, and $\tau_f = -21$ ppm/ $^\circ\text{C}$.¹⁰⁾ In this paper, we investigate the phase evolution, microstructure, and microwave dielectric properties of Na_2O -, Y_2O_3 -, and Ta_2O_5 -doped BMW ceramics, i.e., the $(\text{Ba}_{1-x}\text{Na}_x)(\text{Mg}_{0.5-2x}\text{Y}_{2x}\text{W}_{0.5-x}\text{Ta}_x)\text{O}_3$ system ($0 \leq x \leq 0.05$).

2. Experimental Procedure

Raw powders of BaCO_3 (purity 2N5, Sakai Chem. Ind. Co., Ltd., Japan), MgO (purity 2N, High Purity Chem. Co., Ltd., Japan), Y_2O_3 (purity 4N, High Purity Chem. Co., Ltd., Japan), Na_2CO_3 (purity 2N5, Samcheon Chemical Co., Ltd. Korea), WO_3 (purity 4N, High Purity Chem. Co., Ltd., Japan), and Ta_2O_5 (purity 3N, High Purity Chem. Co., Ltd., Japan) were mixed to prepare the $(\text{Ba}_{1-x}\text{Na}_x)(\text{Mg}_{0.5-2x}\text{Y}_{2x}\text{W}_{0.5-x}\text{Ta}_x)\text{O}_3$ system ($0 \leq x \leq 0.05$). The appropriate ratios of raw powders were ball-milled using zirconia balls and ethyl alcohol in a polyethylene container for 24 h. After drying in an oven, the powder mixture was calcined at 900°C for 10 h in an alumina crucible, followed by pulverizing and uniaxial pressing at 50 MPa to form disk-type specimens 15 mm in diameter. The disk-type specimens were sintered at 1700°C for 1 h. The crystalline phases of the sintered specimens were identified by a powder X-ray diffractometer (XRD, D/MAX-2500V/PC, Rigaku, Japan). The microstructure of the sintered specimens was characterized by a field emission scanning electron microscope (FE-SEM, Quanta

†Corresponding author : Sang-Ok Yoon

E-mail : soyoona@gwnu.ac.kr

Tel : +82-33-640-2361 Fax : +82-33-640-2244

ORCID

<https://orcid.org/0000-0002-1175-3994>

250 FEG, FEI, U.S.A.). Microwave dielectric properties of the specimens were determined using network analyzers. The dielectric constant was measured according to the Hakki–Coleman method using a network analyzer (E5071C, Keysight, U.S.A.). The quality factor was measured by the cavity method using the same equipment. The temperature coefficient of the resonant frequency was measured by the cavity method using a network analyzer (R3767CG, Advantest, Japan) at temperatures ranging from 20°C to 80°C.

3. Results and Discussion

The XRD patterns of Na₂O-, Y₂O₃-, and Ta₂O₅-doped BMW, i.e., (Ba_{1-x}Na_x)(Mg_{0.5-2x}Y_{2x}W_{0.5-x}Ta_x)O₃, ceramics are shown in Fig. 1. All compositions show a 1:1 ordered perovskite structure, i.e., an ordered arrangement of MgO₆ and WO₆ octahedra in the B-site of the perovskite structure. For all compositions, BaWO₄ with low melting point of 1475°C was detected as the secondary phase. It has been

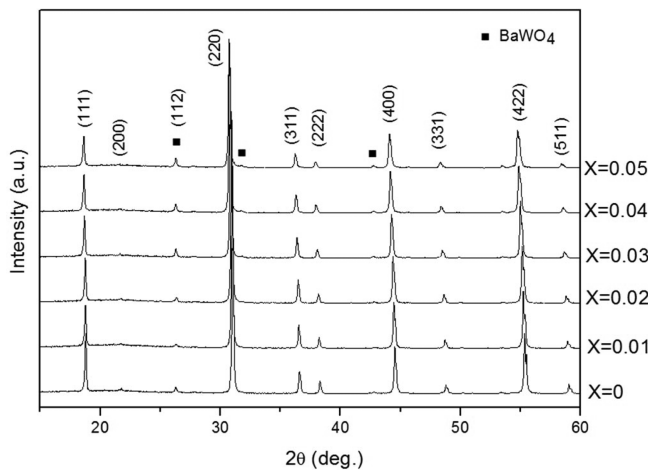


Fig. 1. Powder X-ray diffraction patterns of (Ba_{1-x}Na_x)(Mg_{0.5-2x}Y_{2x}W_{0.5-x}Ta_x)O₃ ceramics.

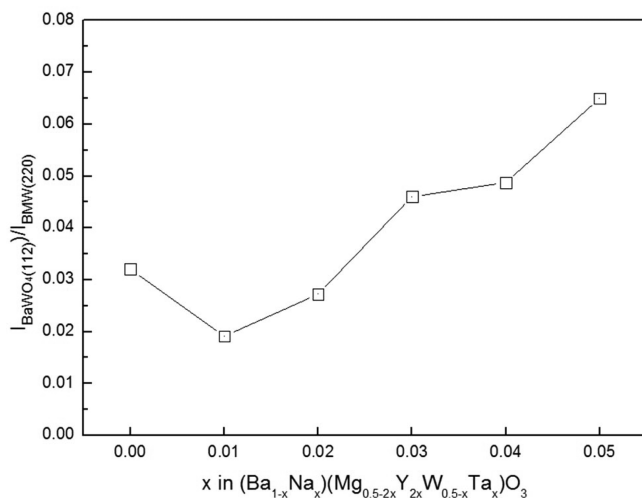


Fig. 2. $I_{\text{BaWO}_4(112)}/I_{\text{BMW}(220)}$ of (Ba_{1-x}Na_x)(Mg_{0.5-2x}Y_{2x}W_{0.5-x}Ta_x)O₃ ceramics.

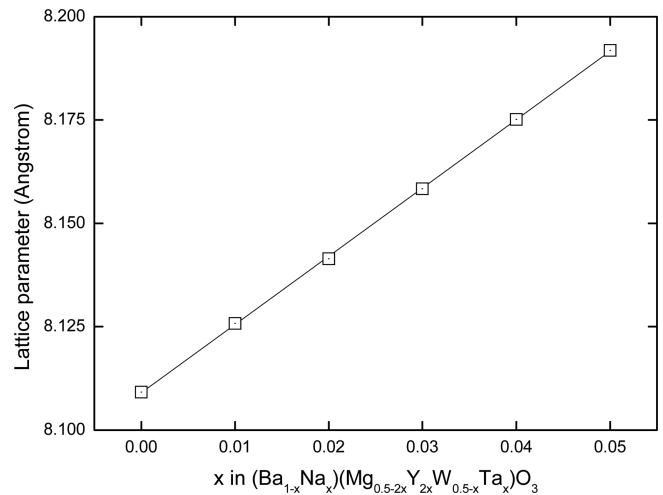


Fig. 3. Lattice parameters of (Ba_{1-x}Na_x)(Mg_{0.5-2x}Y_{2x}W_{0.5-x}Ta_x)O₃ ceramics as a function of x.

reported that BaWO₄ is usually formed during the sintering process of Ba(Mg_{0.5}W_{0.5})O₃ owing to its structural instability at high temperatures.⁸⁻¹⁰ Khalyavin *et al.* proposed the mass balance reaction Ba₂MgWO₆ → BaWO₄ + MgO + BaO as a potential mechanism for the evolution of BaWO₄.¹¹ The intensity ratio of the (112) plane for BaWO₄ to the (220) plane for BMW is shown in Fig. 2. As x increased, the intensity ratio increased, indicating that the addition of the dopants may promote the formation of BaWO₄.

The lattice parameters of (Ba_{1-x}Na_x)(Mg_{0.5-2x}Y_{2x}W_{0.5-x}Ta_x)O₃ ceramics are shown in Fig. 3. As the amount of dopants increased, the lattice parameters of the BMW ceramics increased linearly, indicating the occurrence of a substitutional solid solution. The substitution of Y³⁺ ions larger than that of Mg²⁺, where the ionic radii of Y³⁺ and Mg²⁺ ions are 0.9 Å and 0.72 Å, respectively, when the coordination number is 6, may lead to the increase of lattice parameters. The lattice parameter of undoped BMW ceramics was measured as 8.1092 Å; this value is reasonable because it was reported as between 8.1072 Å (sintered at 1650°C) and 8.1115 Å (at 1600°C).¹¹

The microstructure of the Na₂O-, Y₂O₃-, and Ta₂O₅-doped BMW ceramics was observed by FE-SEM. The typical microstructures (compositions with x = 0.01, 0.03, and 0.05) are shown in Fig. 4. All the compositions exhibited a dense microstructure with polyhedron-shaped grains. In the case of x = 0.05 composition, large grains were observed. According to the EDS result for the x = 0.05 composition as shown in Fig. 4(d), the large grains were identified as BaWO₄. At the sintering temperature of 1700°C, the liquid BaWO₄ contributed to densification.

The variations of linear shrinkage, dielectric constant (ϵ_r), and quality factor ($Q \times f_0$) for the Na₂O-, Y₂O₃-, and Ta₂O₅-doped BMW ceramics are shown in Fig. 5. As x increased, the linear shrinkage increased. The dielectric constant exhibited a tendency to increase slightly as the x value

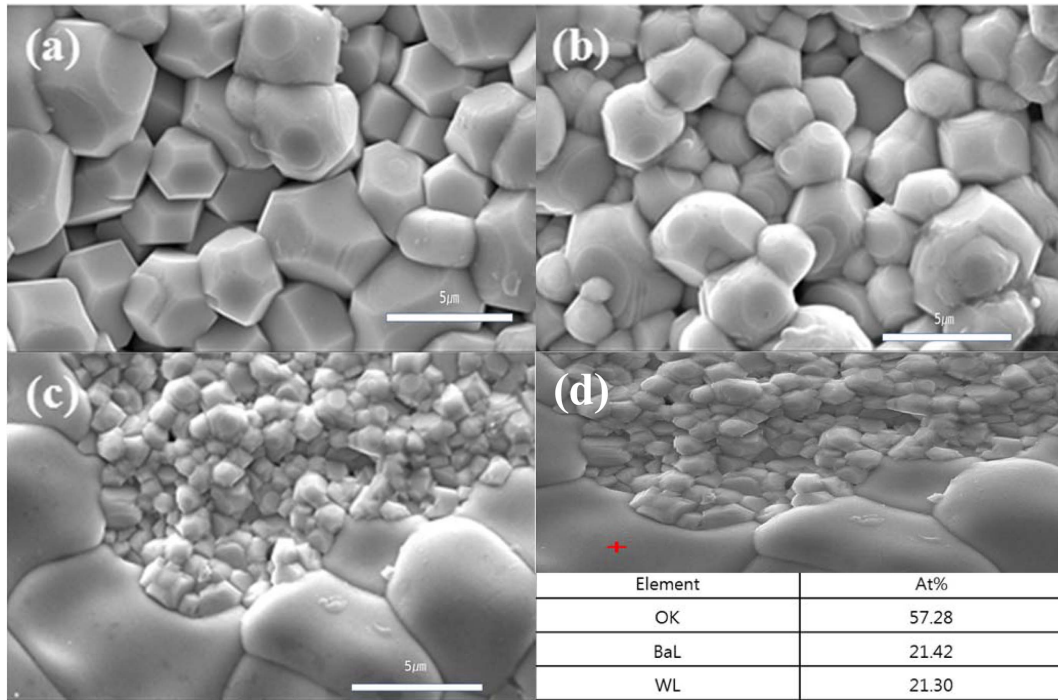


Fig. 4. FE-SEM images of $(\text{Ba}_{1-x}\text{Na}_x)(\text{Mg}_{0.5-2x}\text{Y}_{2x}\text{W}_{0.5-x}\text{Ta}_x)\text{O}_3$ ceramics; (a) $x = 0.01$, (b) $x = 0.03$, (c) $x = 0.05$, and (d) EDS result of large grains for $x = 0.05$.

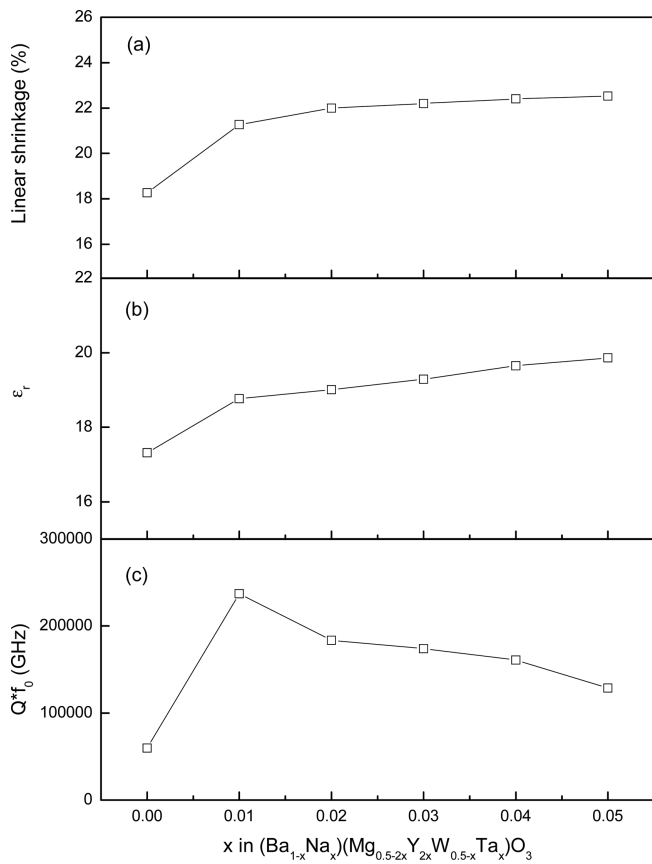


Fig. 5. (a) Linear shrinkage, (b) dielectric constant, and (c) quality factor of $(\text{Ba}_{1-x}\text{Na}_x)(\text{Mg}_{0.5-2x}\text{Y}_{2x}\text{W}_{0.5-x}\text{Ta}_x)\text{O}_3$ ceramics as a function of x .

increased, i.e., with increasing dopant concentration. The dielectric constant is mainly influenced by the relative density and ionic polarizability. The slight increase of the dielectric constant can be attributed to the increase of ionic polarizability by Y_2O_3 and Ta_2O_5 doping; the ionic polarizability of the Y^{3+} ion ($\alpha_{\text{Y}^{3+}} = 3.81 \text{ \AA}^3$) and Ta^{5+} ion ($\alpha_{\text{Ta}^{5+}} = 4.73 \text{ \AA}^3$) is larger than that of the Mg^{2+} ion ($\alpha_{\text{Mg}^{2+}} = 1.31 \text{ \AA}^3$) and W^{6+} ion ($\alpha_{\text{W}^{6+}} = 3.2 \text{ \AA}^3$), respectively.¹²⁾ The quality factor ($Q \times f_0$), i.e., the inverse of the dielectric loss, of undoped BMW was measured as 59,738 GHz, whereas the quality factor of doped BMW has a maximum value of 237,188 GHz in the composition $x = 0.01$, which gradually decreased with increasing x .

The dielectric losses or the inverse of the quality factor were classified into intrinsic and extrinsic categories.¹³⁾ The intrinsic dielectric losses depend on the crystal structure, ac field frequency, and temperature. The extrinsic losses

Table 1. Linear Shrinkage, Lattice Parameters, and Dielectric Properties of $(\text{Ba}_{1-x}\text{Na}_x)(\text{Mg}_{0.5-2x}\text{Y}_{2x}\text{W}_{0.5-x}\text{Ta}_x)\text{O}_3$ Ceramics

x	Linear shrinkage (%)	Lattice parameter, a_0 (Å)	ϵ_t	$Q \times f_0$ (GHz)	τ_f (ppm/°C)
0	18.3	8.1092(3)	17.3	59,738	-27.3
0.01	21.3	8.1260(4)	18.8	237,188	-19.3
0.02	22.0	8.1431(6)	19.0	183,600	-13.9
0.03	22.2	8.1601(14)	19.3	174,078	-12.8
0.04	22.4	8.1781(11)	19.7	160,964	-9.4
0.05	22.5	8.1942(6)	19.9	128,553	-5.6

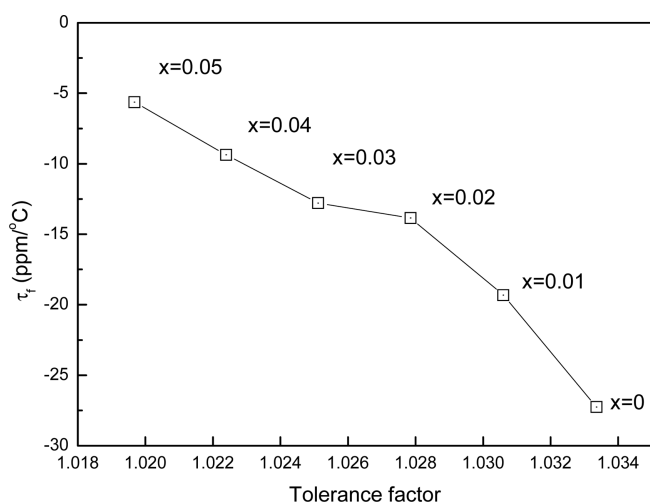


Fig. 6. Temperature coefficient of resonant frequency of $(\text{Ba}_{1-x}\text{Na}_x)(\text{Mg}_{0.5-2x}\text{Y}_{2x}\text{W}_{0.5-x}\text{Ta}_x)\text{O}_3$ ceramics as a function of tolerance of x .

are associated with the microstructure, e.g., pores, grain size, grain boundaries, and secondary phases. Reany and Iddles have pointed out that, in reality, extrinsic losses dominate the quality factor.³⁾ The maximum $Q \times f_0$ value when $x = 0.01$ is attributed to increased density (Fig. 5(a)) and minimum amount of BaWO_4 phase (Fig. 2). The temperature coefficient of resonant frequency (τ_f) as a function of the calculated tolerance factor (t) using Shannon ionic radii is illustrated in Fig. 6.¹⁴⁾ The temperature coefficient of resonant frequency (τ_f) increased monotonically from -19.32 ppm/°C to -5.64 ppm/°C as x increased, i.e., tolerance factor decreased. It is generally considered that the temperature coefficient of resonant frequency of perovskite structures is related to the tolerance factor, i.e., the degree of oxygen octahedral tilting.¹⁵⁾ In the perovskite structure, the temperature coefficient of resonant frequency was reported to be related to the tilting of BO_6 . The tilting of YO_6 was mainly caused by the employment of Y^{3+} (0.9 \AA) with ion radius larger than Mg^{2+} (0.72 \AA). The results of linear shrinkage, lattice parameters, and dielectric properties of $(\text{Ba}_{1-x}\text{Na}_x)(\text{Mg}_{0.5-2x}\text{Y}_{2x}\text{W}_{0.5-x}\text{Ta}_x)\text{O}_3$ ceramics are summarized in Table 1.

4. Conclusions

The phase evolution, microstructure, and microwave dielectric properties of $(\text{Ba}_{1-x}\text{Na}_x)(\text{Mg}_{0.5-2x}\text{Y}_{2x}\text{W}_{0.5-x}\text{Ta}_x)\text{O}_3$ ($0 \leq x \leq 0.05$) ceramics were investigated. In addition to the 1:1 ordered perovskite structure of $\text{Ba}(\text{Mg}_{0.5}\text{W}_{0.5})\text{O}_3$, a secondary phase of BaWO_4 was created. As x increased, the dielectric constant increased slightly and the quality factor showed a tendency to reach the maximum value at $x = 0.01$, and then decreased. The temperature coefficient of resonant frequency (τ_f) increased from -19.32 ppm/°C to -5.64 ppm/°C in the positive direction as x increased. The dielectric constant of the $x = 0.05$ composition was 19.9, the qual-

ity factor was 128,533 GHz, and the temperature coefficient of resonant frequency was -5.6 ppm/°C.

REFERENCES

1. H. Ohsato, T. Tsunooka, M. Ando, Y. Ohishi, Y. Miyauchi, and K. Kakimoto, "Millimeter-Wave Dielectric Ceramics of Alumina and Forsterite with High Quality Factor and Low Dielectric Constant," *J. Korean Ceram. Soc.*, **40** [4] 350–53 (2003).
2. H. Ohsato, M. Ando, and T. Tsunooka, "Synthesis of Forsterite with High Q and Near Zero TC_f for Microwave/Millimeterwave Dielectrics," *J. Korean Ceram. Soc.*, **44** [11] 597–606 (2007).
3. I. M. Reaney and D. Iddles, "Microwave Dielectric Ceramics for Resonators and Filters in Mobile Phone Networks," *J. Am. Ceram. Soc.*, **89** [7] 2063–72 (2006).
4. Y. Zhou, S. Meng, H. Wu, and Z. Yue, "Microwave Dielectric Properties of $\text{Ba}_2\text{Ca}_{1-x}\text{Sr}_x\text{WO}_6$ Double Perovskites," *J. Am. Ceram. Soc.*, **94** [9] 2933–38 (2011).
5. S. Nomura, K. Toyama, and K. Kaneta, "Ba($\text{Mg}_{1/3}\text{Ta}_{2/3}$) O_3 Ceramics with Temperature Stable High Dielectric Constant and Low Microwave Loss," *Jpn. Appl. Phys.*, **21** [10] L624–26 (1982).
6. S. Kawashima, M. Nishida, I. Ueda, and H. Ouchi, "Ba($\text{Zn}_{1/3}\text{Ta}_{2/3}$) O_3 Ceramics with Low Dielectric Loss at Microwave Frequencies," *J. Am. Ceram. Soc.*, **66** [6] 421–23 (1983).
7. H. Takahashi, K. Ayusawa, and N. Sakamoto, "Microwave Dielectric Properties of $\text{Ba}(\text{Mg}_{1/2}\text{W}_{1/2})\text{O}_3$ - BaTiO_3 Ceramics," *Jpn. J. Appl. Phys.*, **36** [9A] 5597–99 (1997).
8. J. J. Bian and J. Y. Wu, "Structure and Microwave Dielectric Properties of B-site Deficient Double Perovskite – $\text{Ba}[(\text{Mg}_{(1-x)/2}\text{Y}_{x/3-x/6})\text{W}_{1/2}]\text{O}_3$," *Ceram. Int.*, **42** [2] 3290–95 (2016).
9. Y.-J. Lin, S.-F. Wang, S.-H. Chen, Y.-L. Liao, and C.-L. Tsai, "Microwave Dielectric Properties of $(\text{Ba}_{1-x}\text{Sr}_x)(\text{Mg}_{0.5}\text{W}_{0.5})\text{O}_3$ Ceramics," *Ceram. Int.*, **41** [7] 8931–35 (2015).
10. J. Y. Wu and J. J. Bian, "Structure Stability and Microwave Dielectric Properties of $(1-x)\text{Ba}(\text{Mg}_{1/2}\text{W}_{1/2})\text{O}_3+x\text{Ba}(\text{Y}_{2/3}\text{W}_{1/3})\text{O}_3$ Ceramics," *J. Am. Ceram. Soc.*, **97** [3] 880–84 (2014).
11. D. D. Khalyavin, J. Han, A. M. R. Senos, and P. Q. Mantas, "Synthesis and Dielectric Properties of Tungsten-Based Complex Perovskites," *J. Mater. Res.*, **18** [11] 2600–7 (2003).
12. R. D. Shannon, "Dielectric Polarizabilities of Ions in Oxides and Fluorides," *J. Appl. Phys.*, **73** [1] 348–66 (1993).
13. N. M. Alford and S. J. Penn, "Sintered Alumina with Low dielectric Loss," *J. Appl. Phys.*, **80** [10] 5895–98 (1996).
14. R. D. Shannon, "Revised Effective Ionic Radii and Systematic Studies of Interatomic Distances in Halides and Chalcogenides," *Acta Cryst.*, **A32** [5] 751–67 (1976).
15. I. M. Reaney, E. L. Colla, and N. Setter, "Dielectric and Structural Characteristics of Ba- and Sr- based Complex Perovskites as a Function of Tolerance Factor," *Jpn. J. Appl. Phys.*, **33** [7A] 3984–90 (1994).